Letters

Practical Design Methodology of IH and IPT Dual-Functional Apparatus

Mina Kim, *Student Member, IEEE*, Hwa-Pyeong Park, *Member, IEEE*, and Jee-Hoon Jung, *Senior Member, IEEE*

***Abstract*—A domestic induction heating (IH) apparatus uses series resonance to transfer the electric energy to the IH vessel. Similarly, an inductive power transfer (IPT) utilizes the resonance to transfer power to the secondary side. Therefore, the IPT function can be integrated into the IH apparatus by sharing the IH power stage as the primary side of the IPT. In this article, a practical design methodology of the IH and IPT (IH-IPT) dual-functional apparatus is proposed. The design considerations of the IPT mode are discussed, such as the power stage design limitation and practical implementation to increase the compatibility to the IH apparatus. Moreover, the design methodology of the IPT mode is provided based on the design considerations. The validity of the proposed design methodology is evaluated through experimental results with an IH-IPT prototype.**

***Index Terms*—Induction heating (IH), inductive power transfer (IPT), resonant power converter.**

I. Introduction

AN INDUCTION heating (IH) apparatus that uses a high-frequency inverter and series resonance has been widely used as a domestic cooking appliance [1], [2]. Similarly, an inductive power transfer (IPT) uses resonance to transfer the power to the secondary side, which is physically separated [3], [4]. Therefore, the IPT function can be integrated into the IH apparatus due to their similarity. In this article, an IH and IPT integrated (IH-IPT) apparatus is proposed with the practical design methodology including the power stage configurations and control scheme. The IPT mode of the IH-IPT apparatus can operate two types of loads: resistive and dc loads. The resistive load generates heat by consuming electric power so that it can be used as a wireless cooker application. Moreover, it can heat the nonferromagnetic vessels, which cannot be heated using the conventional IH apparatus, by using the heat generation of the resistive load. The dc load provides dc power to the secondary side so that it can be used as wireless charging applications. Therefore, the IPT mode can enlarge the applications of the IH apparatus.

Prior existing patents have introduced a conceptual IH and IPT integrated apparatus [5]; however, it requires additional power stage and wireless communication for the IPT function, which decreases the cost-effectiveness of the IH and IPT integrated apparatus. In [6], a switching frequency design method of the IPT system was introduced to provide high power transfer efficiency and output voltage controllability. However, it is only valid for the fixed coupling coefficient, while the IH-IPT apparatus has to operate even under the misalignment condition. In [7] and [8], power stage design methods of the IPT system were introduced to achieve high power transfer efficiency, desired output power, and output voltage controllability. However, the design method in [7] requires an additional power conversion stage at the primary side to provide a constant current power source for the resonant network. Moreover, another design method in [8] needs high-quality factor and coupling coefficient, while the IPT mode of the IH-IPT apparatus has limited quality factor and coupling coefficient due to the fixed power stage configuration of the IH apparatus.

Since the IPT mode of the IH-IPT apparatus has to be integrated into the conventional IH apparatus, the power stage design of the IPT mode has specific design constraints, such as limited primary side current and limited control method. Besides, the IPT mode has to consider the coil misalignment to provide user convenience. In this article, the power stage configurations, control scheme, and resonant network design methodology of the IPT mode are proposed using the design considerations. With the proposed design methodology, the IPT mode of the IH-IPT apparatus can deliver the desired power to the load despite the limited current rating of the conventional IH apparatus. Moreover, it can operate under the coil misalignment condition without any wireless communications, which are used to control the output voltage and power in the conventional IPT system [4]. The validity of the IH-IPT apparatus and the proposed design methodology are evaluated by experimental results with an IH-IPT prototype system, which is developed based on a 2.4-kW IH apparatus.

Manuscript received October 8, 2019; revised December 20, 2019 and January 23, 2020; accepted February 19, 2020. Date of publication February 24, 2020; date of current version May 1, 2020. This work was supported by National Research Foundation of Korea NRF-2019R1A2B5B01069665. *(Corresponding author: Jee-Hoon Jung.)*

Mina Kim is with the School of Electrical and Computer Engineering, Ulsan National Institute of Science and Technology, Ulsan 44919, South Korea (e-mail: kmaop44@unist.ac.kr).

Hwa-Pyeong Park is with the Energy ICT Convergence Research Department, Korea Institute of Energy Research, Daejeon 34129, South Korea (e-mail: hppark@kier.re.kr).

Jee-Hoon Jung is with the School of Electrical and Computer Engineering, Ulsan National Institute of Science and Technology, Ulsan 44919, South Korea (e-mail: jung.jeehoon@gmail.com).

Color versions of one or more of the figures in this letter are available online at http://ieeexplore.ieee.org.

Digital Object Identifier 10.1109/TPEL.2020.2976054

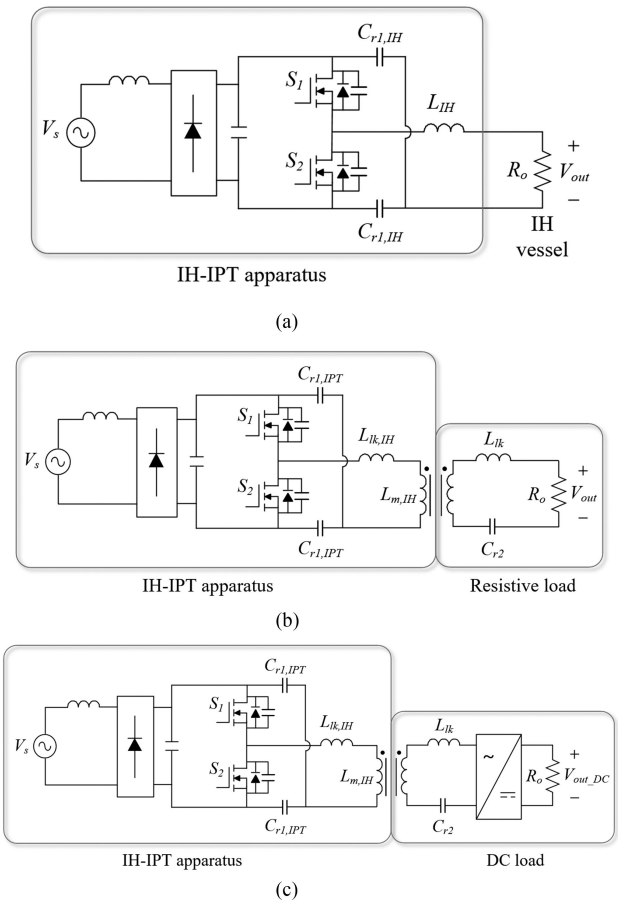

Fig. 1. IH-IPT dual-functional apparatus: (a) IH mode with IH vessel, (b) IPT mode with resistive load, and (c) IPT mode with dc load.

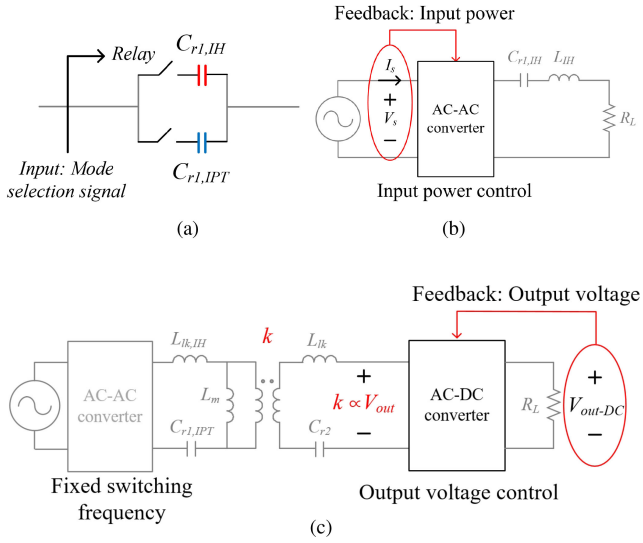

Fig. 2. Control scheme of IH-IPT apparatus: (a) Selective resonant capacitor, (b) IH mode, and (c) IPT mode with dc load.

II. Practical Considerations of IH-IPT Dual-Functional Apparatus

A. Power Stage Configuration

Fig. 1 shows the power stage configurations of the IH-IPT apparatus according to the operating modes. Fig. 1(a) shows the IH mode, which is same as the conventional IH apparatus. Fig. 1(b) and (c) shows the designed power stage of the IPT mode with the resistive and dc loads based on the IH apparatus. The secondary side circuit of the resistive load consists of the resonant network and a variable resistive coil, which adjusts the heat generation to change the temperature. The secondary side circuit of the dc load utilizes an ac–dc converter to provide constant dc power.

The IPT system has plenty of resonant topologies according to the resonance combinations [9]. As the order of the resonance increases, it can achieve wide power transferring distance, low circulating current, and high-power capability. However, the conventional IH system uses the series resonance, which has high cost-effectiveness compared with the complex resonant topologies. Therefore, the primary side of the IPT mode is the series resonant tank. The secondary side design of the IPT mode has two options: series resonance and parallel resonance (so-called SS and SP topologies). In [9], the SS topology with the leakage inductance resonance can provide a constant output voltage. The SS topology with the self-inductance resonance and the SP topology can provide a constant output current. However, the constant output current type topologies can cause a safety issue because the output voltage of them diverges under the open load condition. Therefore, the SS topology with the leakage inductance resonance is selected as the IPT mode of the IH-IPT apparatus due to its natural protection feature.

B. Control Method

Fig. 2 shows the operating mode change and the control method according to the operating mode of the IH-IPT apparatus. Fig. 2(a) shows the selective resonant capacitor of the IH-IPT apparatus using a relay circuit. The selective resonant capacitor can be designed based on the desired switching frequency of each operating mode. The IH mode regulates the input power according to the desired power, as shown in Fig. 2(b). On the other hand, the IPT mode operates as a fixed switching frequency, which is the series resonant frequency to obtain the constant output voltage, as shown in Fig. 2(c). The output voltage of the resonant network of the IPT mode (V_{out}) is proportional to the coupling coefficient under the misalignment condition. Although V_{out} is reduced, the ac–dc converter can regulate the constant output voltage. The control scheme of the dc load does not require the communication between the primary and secondary sides. If V_{out} becomes lower than the minimum input voltage of the ac–dc converter, the IPT mode with the dc load cannot operate. Therefore, the resonant network should be designed to provide enough voltage to the load under the maximum misalignment condition.

C. Current Limitation

The primary side current of the IPT mode is limited due to the IH apparatus design. The primary side current of the IPT mode

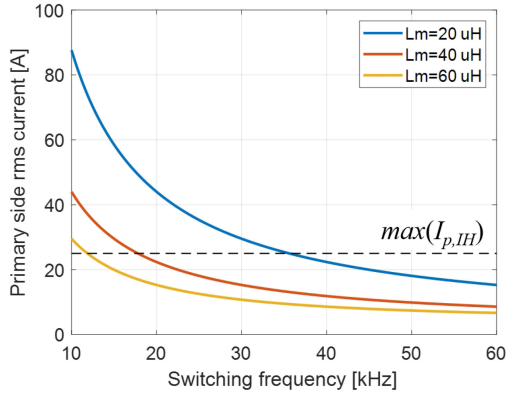

Fig. 3. RMS value of primary side current at IPT mode according to switching frequency with different magnetizing inductance.

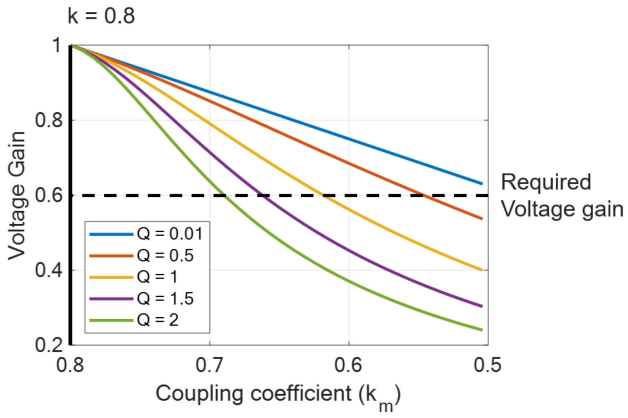

Fig. 4. Voltage gain curves under misalignment conditions according to Q and k_m.

at the resonant frequency can be expressed as follows:

$$Z_{\text{in}} = \frac{j\omega_r L_{m,\text{IH}} R_o}{j\omega_r L_{m,\text{IH}} + R_o} \tag{1}$$

$$I_{p,\text{IPT}} = \left|\frac{V_{\text{in}}}{Z_{\text{in}}}\right| = V_{\text{in}}\sqrt{\frac{1}{\left(\omega_r L_{m,\text{IH}}\right)^2} + \frac{1}{R_o^2}} \tag{2}$$

where Z_{in} is the input impedance of the resonant network, ω_r is the series resonant frequency, V_{in} is the effective input voltage applied to the resonant network, and R_o is the primary side referred load resistance. Fig. 3 shows the primary side current of the IPT mode. Both the high switching frequency and magnetizing inductance can suppress the primary side current. However, the magnetizing inductance is practically limited. Moreover, high switching frequency increases the coil losses and the quality factor, which decreases V_{out}. Therefore, a proper switching frequency is required to satisfy the current rating and the required output voltage of the resonant network.

III. IPT Mode Design

The resonant frequency design for the IPT mode is significant to satisfy two factors: 1) current rating, and 2) V_{out} under the misalignment condition. The minimum and maximum switching frequencies are determined by 1) and 2), respectively. As shown in Fig. 3, the minimum switching frequency can be obtained by following equation not to exceed the current limitation

$$2\pi f_s > \omega_{r,\min} = \frac{1}{L_m\sqrt{\frac{I_{p,\text{IH}}^2}{V_{\text{in}}^2} - \frac{1}{R_o^2}}} \tag{3}$$

where $\omega_{r,\min}$ is minimum switching (resonant) frequency to satisfy the current rating.

At the misalignment condition, the voltage gain of the resonant network under the misalignment condition can be obtained as

$$G_{v,m}|_{2\pi f_s=\omega_r} = \frac{V_{\text{out}}}{V_{\text{in}}} = \left[\left(\frac{k}{k_m}\right)^2 + \left\{Qk_m\left(\frac{k}{k_m}-1\right)\left(\frac{k}{k_m}+1\right)\right\}^2\right]^{-\frac{1}{2}} \tag{4}$$

where $G_{v,m}$ is the voltage gain at the misalignment condition, k and k_m are the coupling coefficient at perfect alignment and the misalignment condition, respectively, and Q is the quality factor of the resonant network ($Q = \omega_r L_{\text{self}}/R_o$).

Fig. 4 shows the voltage gain under the misalignment condition according to Q and k_m. The vertical solid line denotes the coupling coefficient at the alignment condition (k). As k_m decreasing, the voltage gains decrease. Moreover, the voltage gain with the high-quality factor decreases more than that with the low-quality factor despite the same coupling coefficient. Therefore, the design method for both k_m and Q is required to preserve the output voltage of the resonant network under the misalignment condition. The key equation to design k_m and Q can be expressed as follows:

$$\frac{k_m}{k} > \frac{V_{o,\text{req}}}{V_{\text{in}}} \tag{5}$$

$$Q < \frac{1}{k_m\left(\frac{k}{k_m}-1\right)\left(\frac{k}{k_m}+1\right)}\sqrt{\left(\frac{V_{in}}{V_{o,\text{req}}}\right)^2 - \left(\frac{k}{k_m}\right)^2} \tag{6}$$

where $V_{o,\text{req}}$ is the required output voltage. From (7) and the definition of Q, the maximum switching frequency is derived as follows:

$$2\pi f_s < \omega_{r,\max} = \frac{R_o}{L_{\text{self}}} \cdot \frac{1}{k_m\left(\frac{k}{k_m}-1\right)\left(\frac{k}{k_m}+1\right)}\sqrt{\left(\frac{V_{in}}{V_{o,\text{req}}}\right)^2 - \left(\frac{k}{k_m}\right)^2} \tag{7}$$

where $\omega_{r,\max}$ is maximum switching frequency to provide the required output voltage at the misalignment condition.

Consequently, the switching frequency of the IPT mode can be designed using (3) and (7). Besides, the resonant capacitor of the IPT mode can be designed based on the switching frequency because the leakage inductance of the IPT mode is already determined by the coil specification and the airgap. Fig. 5 shows the available switching frequency region according to the output

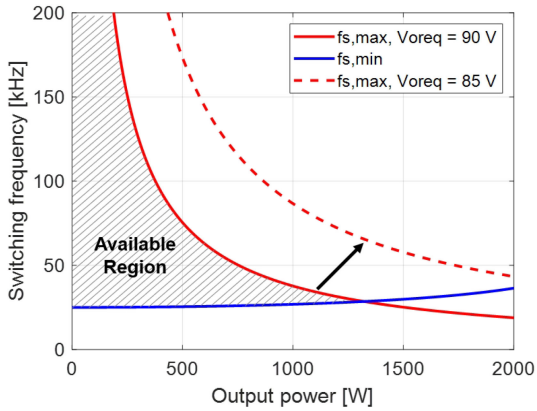

Fig. 5. Available switching frequency region of IPT mode.

TABLE I
IH-IPT PROTOTYPE APPARATUS DESIGN PARAMETERS

Parameters	Value
Turn number of coil	16
Radius/Airgap	100 mm/20 mm
Self-inductance	49.46 μH
IH mode power	2.4 kW
IPT mode power	Resistive load: 1.5 kW/ DC load: 500 W
Effective load and quality factor of load types	Resistive load: 7 Ω, 1.33/ DC load: 20 Ω, 0.47
$V_{o,req}$	90 V
k and k_m (lateral misalignment)	0.6158/ 0.5304 (30 mm)
$C_{r1,IH}$ and $C_{r1,IPT}$	1.36 μF/ 1.5 μF
Switching frequency range by (3) and (7)	[27.43 kHz, 53.72 kHz]
Switching frequency of IPT mode	30 kHz

power of the IPT mode. The available region decreases as the output power of the IPT mode increases. The available region and the power capacity of the IPT mode can be extended by decreasing the required output voltage or increasing coupling coefficient under the worst misalignment condition and the current rating of the original IH system. The dashed line in Fig. 5 shows the extension of the available region by decreasing the required output voltage.

IV. EXPERIMENTAL RESULTS

Table I shows the designed parameters of the IH-IPT prototype. The power capacity of the resistive and dc loads are selected based on power demand of the loads. The power capacities of the loads can be redesigned using (3) and (7). Fig. 6 shows the operating waveforms of the IH and IPT modes of the IH-IPT apparatus. Since the switching frequency is the series resonant frequency, the zero-voltage switching and soft commutation can be provided. Besides, the input voltage of the ac–dc converter has only grid frequency components, as shown in Fig. 6(c), so that the power factor correction circuit can be used as the ac–dc converter.

Fig. 7 shows V_{out} reduction according to the coupling coefficient under the misalignment condition. The switching frequency and Q are designed to satisfy the target performance, which is expressed with the red graph. The solid line is theoretical expectation of the output voltage. The dashed line is practical

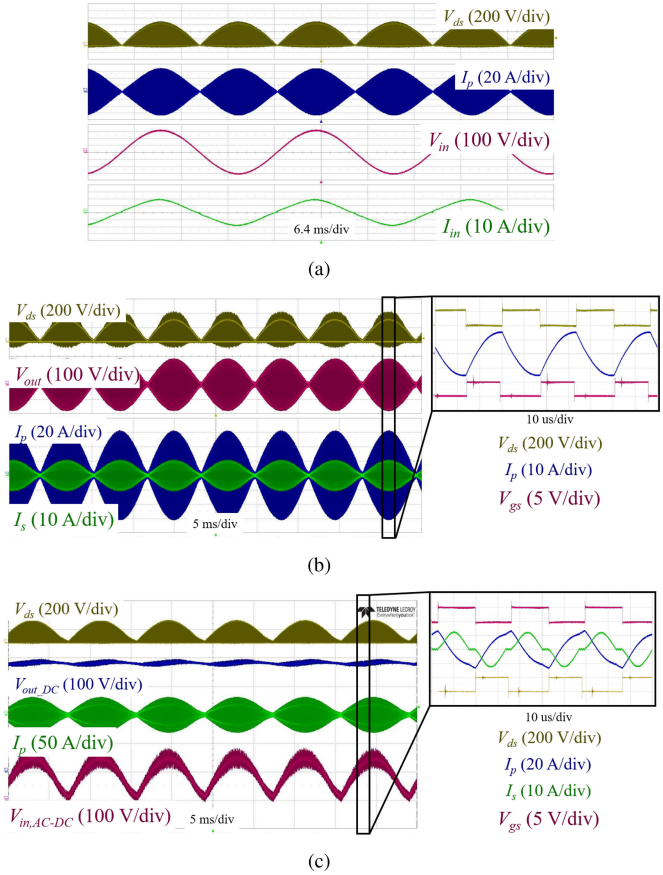

Fig. 6. Operating waveforms of IH-IPT apparatus: (a) IH mode, (b) resistive load, and (c) dc load of IPT modes.

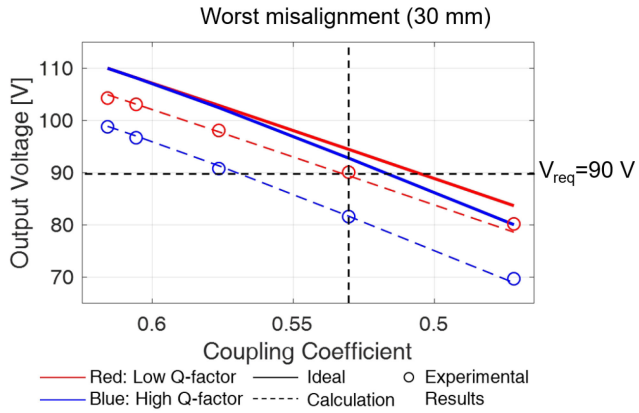

Fig. 7. V_{out} reduction curves according to coupling coefficient under misalignment condition.

expectation of the output voltage, which considers the voltage drop from the conduction losses. The markers are the measured output voltage through the experiments. The output voltage can be preserved as higher than the required output voltage at the worst misalignment condition.

Fig. 8 shows the power transfer efficiency of the IPT mode. The dashed line shows the theoretical expectations of the power transfer efficiency, which considers the switching and conduction losses from the circuit. The resistive load has higher power

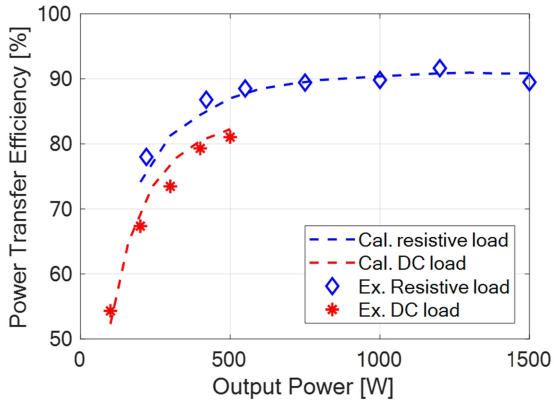

Fig. 8. Power transfer efficiency of IPT mode according to output power.

transfer efficiency than the dc load case because the dc load has the additional losses from the ac–dc converter and the dc load operates at the light load condition of the IH-IPT apparatus. The maximum efficiency is 91.64% and 81.04% in the case of the resistive load and the dc load, respectively.

V. Conclusion

In this research, the practical design methodology for the IH-IPT apparatus is proposed to implement the IPT mode using the conventional IH apparatus. The IPT mode of the IH-IPT apparatus, which can cope with both the resistive and dc loads, can enhance the IH apparatus by providing additional applications. To implement the IPT mode based on the IH apparatus with its primary side circuit, the power stage configurations are proposed according to the load types. Moreover, the SS topology of the IPT mode can provide not only the constant voltage according to the load variations but also the natural protection at the open load condition. However, the IPT mode has to suppress the primary side current and increases the output voltage under the misalignment condition to provide wide operation. The analysis results of the resonant network show that high switching frequency can suppress the primary side current while low switching frequency can preserve the output voltage of the resonant network under the misalignment condition. Therefore, the resonant network design provides the proper switching frequency of the IPT mode, which can satisfy the two requirements simultaneously. Finally, the experimental results show the feasibility of the IH-IPT apparatus with the proposed design methodology. The IH-IPT prototype developed using the conventional IH apparatus can operate under the IPT mode at 1.5 kW with the resistive load and at 500 W with the dc load. The proposed system can operate under the 30 mm lateral misalignment condition, which is designed as the maximum lateral misalignment. Besides, the maximum power transfer efficiency of the IPT mode is 91.64% and 81.04% for the resistive load and the dc load, respectively.

References

[1] H. Sarnago, O. Lucía, A. Mediano, and J. M. Burdío, "Class-d/de dual-mode-operation resonant converter for improved-efficiency domestic induction heating system," *IEEE Trans. Power Electron.*, vol. 28, no. 3, pp. 1274–1285, Mar. 2013.

[2] J. M. Burdio, F. Monterde, J. R. Garcia, L. A. Barragan, and A. Martinez, "A two-output series-resonant inverter for induction-heating cooking appliances," *IEEE Trans. Power Electron.*, vol. 20, no. 4, pp. 815–822, Jul. 2005.

[3] X. Lu, P. Wang, D. Niyato, D. I. Kim, and Z. Han, "Wireless charging technologies: Fundamentals, standards, and network applications," *IEEE Commun. Surveys Tut.*, vol. 18, no. 2, pp. 1413–1452, Apr.–Jun. 2016.

[4] S. Li and C. C. Mi, "Wireless power transfer for electric vehicle applications," *IEEE J. Emerg. Sel. Topics Power Electron.*, vol. 3, no. 1, pp. 4–17, Mar. 2015.

[5] E. S. Kim, H. Moon, and Y. K. Kim, "Induction heating and wireless power transferring device," Patent KR20 180 085 319.

[6] W. Zhang, S. Wong, C. K. Tse, and Q. Chen, "Design for efficiency optimization and voltage controllability of seriesseries compensated inductive power transfer systems," *IEEE Trans. Power Electron.*, vol. 29, no. 1, pp. 191–200, Jan. 2014.

[7] Y. H. Sohn, B. H. Choi, E. S. Lee, G. C. Lim, G. Cho, and C. T. Rim, "General unified analyses of two-capacitor inductive power transfer systems: Equivalence of current-source SS and SP compensations," *IEEE Trans. Power Electron.*, vol. 30, no. 11, pp. 6030–6045, Nov. 2015.

[8] Y. Frechter and A. Kuperman, "Output voltage range of a power loaded series-series compensated inductive wireless power transfer link operating in load-independent regime," *IEEE Trans. Power Electron.*, vol. 35, no. 6, pp. 6586–6593, Jun. 2020.

[9] W. Zhang and C. C. Mi, "Compensation topologies of high-power wireless power transfer systems," *IEEE Trans. Veh. Technol.*, vol. 65, no. 6, pp. 4768–4778, Jun. 2016.